There are many applications of the rectilinearity measure in a number of areas. For example, *3D shape retrieval* and *pose normalization*.

The explosion in the number of available 3D models has led to the development of 3D shape retrieval systems that, given a query object, retrieve similar 3D objects [23]. Therefore, "Shape-based 3D Model Retrieval" methodology, concentrating on the representation, recognition and matching of 3D models based on their intrinsic shapes, has become a new hot topic in computer vision [27]. A growing number of researchers have been involved in this area, and have already made much progress. Feature extraction is the key issue for an efficient retrieval system and a considerable number of shape descriptors [3], such as: D1 [1], D2 [14], spherical harmonic descriptor [11], skeleton based shape descriptor [22], and view based features [4] *et al* have been proposed. These signatures, which describe the global geometrical shapes of 3D models, intrinsically have limitations on their discriminating capability as well as their effectiveness and efficiency. Consequently, many people have introduced partial matching schemes and shape descriptors with local information [23, 27, 7] in order to improve retrieval performance. However, such schemes are usually much more computationally expensive and thus not suitable for real time systems. Intuitively, the combination of different kinds of descriptors could be an alternative choice.

Because a large number of shape descriptors are not invariant under similarity transformations (scaling, translation and rotation) pose normalization is often necessary during the preprocessing stages of 3D shape retrieval systems. To normalize a 3D model for scale, the average distance of the points on its surface to the center of mass should be scaled to a constant, while the translation invariance is accomplished by translating the center of mass to the origin. Securing the scale and the translation invariance is trivial but not the rotation invariance. The most prominent tool for accomplishing the rotation invariance is Principal Component Analysis (PCA) [25, 15, 26, 6]. The PCA algorithm is fairly simple and efficient. However, it may erroneously assign the principal axes and produce inaccurate normalization results, especially when the eigenvalues are equal or close to each other, which is its intrinsic drawback that cannot be overcome easily [24]. Therefore, we suggest using rectilinearity, symmetry, etc for estimating pose.

In this paper, we describe, prove and test a novel rectilinearity measurement for 3D meshes. Two examples of its applications are also carried out. Following this introduction, the remainder of the paper is organized as follows. In Section 2, we describe the definition and some concepts of the rectilinearity of 3D meshes. Then, the basic idea of the rectilinearity measurement is briefly introduced in Section 3 where corresponding theorems are also explicitly proved. Section 4 defines a novel rectilinearity measurement for 3D meshes. This is followed by description about how to use a GA to calculate the approximate rectilinearity of 3D meshes in section 5. Afterwards, Section 6 illustrates some experimental results which validate the effectiveness and robustness of our shape measurement. Furthermore, two applications on 3D shape retrieval and pose registration are carried out in Section 7. Finally, we provide the conclusion of this paper as well as some future research directions in Section 8.

## 2. DEFINITION AND NOTATIONS

In this section, we first describe a formal definition of rectilinear 3D meshes and then give some notations used in this paper. For convenience, the meshes we describe here are 3D triangle meshes, but the following definitions and theorems can also be adopted to other 3D polygon meshes.

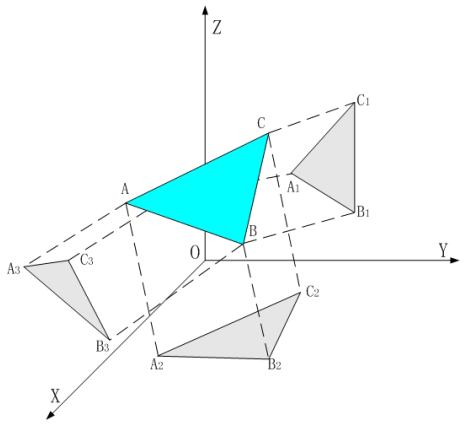


**Figure 1: Projecting a triangle on three orthogonal planes**

DEFINITION 1. *A 3D mesh $M$ is rectilinear if the angles, between the normals of every two faces, belong to $\{0, \frac{\pi}{2}, \pi, \frac{3\pi}{2}\}$.*

Given a 3D mesh $M$ which consists of $N$ triangles $\{T_1, T_2, \ldots, T_N\}$, the surface area of the mesh $M$ is represented as $S(M)$, while three projected areas corresponding to the $YOZ$, $ZOX$ and $XOY$ planes are $P_x(M), P_y(M), P_z(M)$, respectively, defined by

$$P_x(M) = \sum_{i=1}^{N} S_{ix}, \;\; P_y(M) = \sum_{i=1}^{N} S_{iy}, \;\; P_z(M) = \sum_{i=1}^{N} S_{iz}.$$

where $S_{ix}, S_{iy}, S_{iz}$ are the projected areas of triangle $T_i$ on the plane $YOZ$, $ZOX$ and $XOY$, respectively (see Figure 1).

If we rotate the coordinate frame, we will get new projected areas of the mesh $M$. Therefore, we will use $P_x(M,\alpha,\beta,\gamma)$, $P_y(M,\alpha,\beta,\gamma)$, $P_z(M,\alpha,\beta,\gamma)$ for these three projected areas which are obtained after successively rotating the coordinate frame around its $x, y, z$ axes by angles $\alpha, \beta, \gamma$. Here we denote the sum of these three projected areas by

$$P(M,\alpha,\beta,\gamma) = \sum_{i=1}^{N} P(T_i,\alpha,\beta,\gamma)$$

$$= P_x(M,\alpha,\beta,\gamma) + P_y(M,\alpha,\beta,\gamma) + P_z(M,\alpha,\beta,\gamma)$$

where $P(T_i,\alpha,\beta,\gamma) = S'_{ix} + S'_{iy} + S'_{iz}$ is the sum of three projected areas $(S'_{ix}, S'_{iy}, S'_{iz})$ of the triangle $T_i$ in the rotated coordinate frame.

Let that the original coordinates of the vertices of the triangles $\{T_1, T_2, \ldots, T_N\}$ be denoted by $(x_{i0}, y_{i0}, z_{i0})$, $(x_{i1}, y_{i1}, z_{i1})$, $(x_{i2}, y_{i2}, z_{i2})$, $i = 1, \ldots, N$. After successively rotating the coordinate frame around its $x, y, z$ axes with angles $\alpha, \beta, \gamma$, we get their new coordinates, represented as $(x'_{i0}, y'_{i0}, z'_{i0})$, $(x'_{i1}, y'_{i1}, z'_{i1})$, $(x'_{i2}, y'_{i2}, z'_{i2})$, $i = 1, \ldots, N$, specified by formulae

$$(x'_{ij}, y'_{ij}, z'_{ij})^T = R(\alpha,\beta,\gamma)(x_{ij}, y_{ij}, z_{ij})^T, i = 1, \ldots, N, j = 0, 1, 2$$

where $R(\alpha,\beta,\gamma)$ stands for the rotation matrix. Let

$$\overrightarrow{X}_{ij} = (x_{ij}, y_{ij}, z_{ij}), \overrightarrow{X'}_{ij} = (x'_{ij}, y'_{ij}, z'_{ij}), i = 1, \ldots, N; j = 0, 1, 2.$$

Define

$$\overrightarrow{\eta'}_i = (\eta'_{ix}, \eta'_{iy}, \eta'_{iz}) = (\overrightarrow{X'}_{i1} - \overrightarrow{X'}_{i0}) \times (\overrightarrow{X'}_{i2} - \overrightarrow{X'}_{i0}).$$

Then, the area of the triangle $T_i$ is

$$S_i = S'_i = \frac{1}{2}|\overrightarrow{\eta'}_i| = \frac{1}{2}\sqrt{(\eta'_{ix})^2 + (\eta'_{iy})^2 + (\eta'_{iz})^2}$$

and the projected areas of triangle $T_i$ on the plane $YOZ$, $ZOX$ and $XOY$ are

$$S'_{ix} = \frac{1}{2}|\eta'_{ix}|, S'_{iy} = \frac{1}{2}|\eta'_{iy}|, S'_{iz} = \frac{1}{2}|\eta'_{iz}|,$$

respectively. Thus, We have

$$S_i = \sqrt{(S'_{ix})^2 + (S'_{iy})^2 + (S'_{iz})^2} \leq S'_{ix} + S'_{iy} + S'_{iz}.$$

Using Root Mean Square-Arithmetic Mean Inequality, we obtain

$$S'_{ix} + S'_{iy} + S'_{iz} \leq \sqrt{3}\sqrt{(S'_{ix})^2 + (S'_{iy})^2 + (S'_{iz})^2} = \sqrt{3}S_i.$$

Thus $S_i \leq S'_{ix} + S'_{iy} + S'_{iz} \leq \sqrt{3}S_i$. Since

$$S(M) = \sum_{i=1}^{N} S_i = \sum_{i=1}^{N} \sqrt{(S'_{ix})^2 + (S'_{iy})^2 + (S'_{iz})^2},$$

$$P(M,\alpha,\beta,\gamma) = \sum_{i=1}^{N} \left(S'_{ix} + S'_{iy} + S'_{iz}\right).$$

Finally, we get

$$S(M) \leq P(M,\alpha,\beta,\gamma) \leq \sqrt{3}S(M).$$

THEOREM 1. *A given 3D mesh $M$ is rectilinear if and only if there exists a choice of the coordinate system such that the surface area of $M$ and the sum of three projected areas of $M$ coincide, i.e.*

$$S(M) = P(M,\alpha,\beta,\gamma)$$

*for some $\alpha,\beta,\gamma \in [0,2\pi]$.*

PROOF. On the one hand, if $M$ is rectilinear then a rotation of coordinate frame, such that all faces of $M$ become parallel to one of three planes $YOZ$, $ZOX$, $XOY$, ensures the equality $S(M) = P(M,\alpha,\beta,\gamma)$, where $\alpha,\beta,\gamma$ are the rotation angles. On the other hand, $S(M) = P(M,\alpha,\beta,\gamma)$ implies

$$\sum_{i=1}^{N} \sqrt{(S'_{ix})^2 + (S'_{iy})^2 + (S'_{iz})^2} = \sum_{i=1}^{N} \left(S'_{ix} + S'_{iy} + S'_{iz}\right).$$

Furthermore, we derive

$$\sqrt{(S'_{ix})^2 + (S'_{iy})^2 + (S'_{iz})^2} = S'_{ix} + S'_{iy} + S'_{iz}$$

$$\Rightarrow S'_{ix}S'_{iy} + S'_{iy}S'_{iz} + S'_{iz}S'_{ix} = 0, i = 1,\ldots,N.$$

Therefore at least two of three projected areas $S'_{ix}, S'_{iy}, S'_{iz}$ of a triangle $T_i$ are 0, which means all triangles $T_i (i = 1,\ldots,N)$ of the given mesh $M$ are parallel to one of these three planes $YOZ$, $ZOX$, $XOY$, namely, every triangle is parallel or orthogonal to all other triangles, i.e. $M$ is rectilinear. □

## 3. THE BASIC IDEA

Theorem 1 gives the basic idea for the rectilinearity measurement of 3D meshes. Theorem 1 together with $S(M) \leq P(M,\alpha,\beta,\gamma)$ suggests that the ratio

$$\max_{\alpha,\beta,\gamma\in[0,2\pi]} \frac{S(M)}{P(M,\alpha,\beta,\gamma)}$$

can be used as a rectilinearity measure, which is invariant under similarity transformations, for the mesh $M$.

Since $S(M) \leq P(M,\alpha,\beta,\gamma)$, it follows that $\frac{S(M)}{P(M,\alpha,\beta,\gamma)} \leq 1$. However, the infimum for the set of values of $\frac{S(M)}{P(M,\alpha,\beta,\gamma)}$ is not zero. So, for our purpose, it is necessary to determine the maximal possible $\mu$ such that $\max_{\alpha,\beta,\gamma\in[0,2\pi]} \frac{S(M)}{P(M,\alpha,\beta,\gamma)}$ belongs to the interval $[\mu, 1]$ for any mesh $M$. Theorem 2 shows that $\mu = \frac{2}{3}$ and there is no mesh satisfying

$$\max_{\alpha,\beta,\gamma\in[0,2\pi]} \frac{S(M)}{P(M,\alpha,\beta,\gamma)} = \frac{2}{3}.$$

THEOREM 2. *1) The inequality*

$$\max_{\alpha,\beta,\gamma\in[0,2\pi]} \frac{S(M)}{P(M,\alpha,\beta,\gamma)} > \frac{2}{3}$$

*holds for any 3D mesh $M$.*
*2) For any $\varepsilon > 0$, there is a mesh $M$ such that*

$$\max_{\alpha,\beta,\gamma\in[0,2\pi]} \frac{S(M)}{P(M,\alpha,\beta,\gamma)} < \frac{2}{3} + \varepsilon$$

*or equivalently*

$$\inf\left\{\max_{\alpha,\beta,\gamma\in[0,2\pi]} \frac{S(M)}{P(M,\alpha,\beta,\gamma)}\right\} = \frac{2}{3}.$$

PROOF. For convenience, we use an alternative expression of $P(M,\alpha,\beta,\gamma)$ by

$$\begin{aligned} P(M,\alpha,\beta,\gamma) &= \sum_{i=1}^{N} P(T_i,\alpha,\beta,\gamma) \\ &= \sum_{i=1}^{N} P(T_i,\psi_i(\alpha,\beta,\gamma),\varphi_i(\alpha,\beta,\gamma)) \\ &= \sum_{i=1}^{N} \Big(|\cos(\psi_i(\alpha,\beta,\gamma))|S_i \\ &\quad +|\sin(\psi_i(\alpha,\beta,\gamma))||\cos(\varphi_i(\alpha,\beta,\gamma))|S_i \\ &\quad +|\sin(\psi_i(\alpha,\beta,\gamma))||\sin(\varphi_i(\alpha,\beta,\gamma))|S_i\Big) \end{aligned}$$

where $\psi_i(\alpha,\beta,\gamma)$ denotes the angle between the $z$ axis and the normal of triangle $T_i$ after the coordinate frame has rotated by the angles $\alpha,\beta,\gamma$ around its $x,y,z$ axes, while the angle between the $x$ axis and the perpendicular plane of $T_i$ is represented by $\varphi_i(\alpha,\beta,\gamma)$. (See Figure 2). For simplicity of notation, we will use $\psi_i$ and $\varphi_i$ instead of $\psi_i(\alpha,\beta,\gamma)$ and $\varphi_i(\alpha,\beta,\gamma)$ in the following part of this paper.

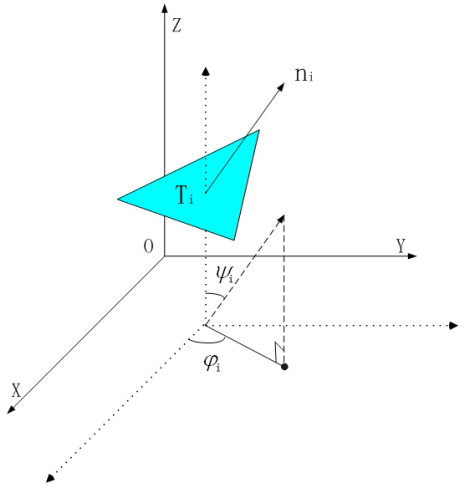


**Figure 2: Geometric relationships between a triangle and the coordinate system**

We prove the statement 1) by a contradiction. Let us assume the contrary, i.e., there exists a mesh $M$, which consists of $N$ triangles, such that $\frac{S(M)}{P(M,\alpha,\beta,\gamma)} \leq \frac{2}{3}$, or equivalently, $\frac{P(M,\alpha,\beta,\gamma)}{S(M)} \geq \frac{3}{2}$, for any $\alpha,\beta,\gamma \in [0,2\pi]$.

Since $\frac{P(M,\alpha,\beta,\gamma)}{S(M)}$ is a continuous nonconstant function defining on $\alpha,\beta,\gamma \in [0,2\pi]$, the equality $\frac{P(M,\alpha,\beta,\gamma)}{S(M)} = \frac{3}{2}$ cannot be always satisfied for all $\alpha,\beta,\gamma \in [0,2\pi]$. (see Appendix Lemma 1). So we have

$$\begin{aligned}
&\iint_{\Sigma} \frac{P(M,\alpha,\beta,\gamma)}{S(M)} \cdot ds \\
= &\iint_{\Sigma} \frac{\sum_{i=1}^{N} P(T_i,\psi_i,\varphi_i)}{S(M)} \cdot ds \\
= &\sum_{i=1}^{N} \int_0^{2\pi} \int_0^{\pi} \frac{P(T_i,\psi_i,\varphi_i)}{S(M)} \cdot \sin\psi_i d\psi_i d\varphi_i \\
= &\int_0^{2\pi} \int_0^{\pi} \frac{\sum_{i=1}^{N} P(T_i,\psi,\varphi)}{S(M)} \cdot \sin\psi d\psi d\varphi \\
> &\iint_{\Sigma} \frac{3}{2} \cdot ds \\
= &\int_0^{2\pi} \int_0^{\pi} \frac{3}{2} \cdot \sin\psi d\psi d\varphi = 6\pi
\end{aligned}$$

where $\Sigma$ denotes the surface of the unit sphere. Using the last inequality, we derive

$$\begin{aligned}
6\pi < &\int_0^{2\pi} \int_0^{\pi} \frac{\sum_{i=1}^{N} P(T_i,\psi,\varphi)}{S(M)} \cdot \sin\psi d\psi d\varphi \\
= &\frac{1}{S(M)} \sum_{i=1}^{N} \int_0^{2\pi} \int_0^{\pi} P(T_i,\psi,\varphi) \cdot \sin\psi d\psi d\varphi \\
= &\frac{1}{S(M)} \sum_{i=1}^{N} \int_0^{2\pi} \int_0^{\pi} (|\cos\psi| + |\sin\psi||cos\varphi| \\
&+|\sin\psi||sin\varphi|) S_i \sin\psi d\psi d\varphi \\
= &\frac{\sum_{i=1}^{N} S_i \int_0^{\pi} (2\pi|\cos\psi|\sin\psi + 8|\sin\psi|^2) d\psi}{\sum_{i=1}^{N} S_i} \\
= &\frac{\sum_{i=1}^{N} S_i (2\pi + 4\int_0^{\pi} (2\sin^2\psi - 1 + 1) d\psi)}{\sum_{i=1}^{N} S_i} \\
= &\frac{\sum_{i=1}^{N} (6\pi) S_i}{\sum_{i=1}^{N} S_i} = 6\pi.
\end{aligned}$$

This yields the contradiction $6\pi < 6\pi$ which proves 1).

It is enough to prove the statement 2) if we can find a sequence of meshes $\ldots M_{99}, M_{100}, \ldots, M_n, \ldots$ ($M_n$ denotes a mesh consisting of $n$ triangles) such that

$$\lim_{n\to\infty} \left( \max_{\alpha,\beta,\gamma\in[0,2\pi]} \frac{S(M_n)}{P(M_n,\alpha,\beta,\gamma)} \right) = \frac{2}{3}$$

Intuitively the sequence of $n$-triangles mesh $M_n$ inscribed into the unit sphere satisfies the previous equality. According to the properties of the sphere, we get the surface area $\lim_{n\to\infty} S(M_n) = 4\pi$ and the sum of three projected areas $\lim_{n\to\infty} P(M_n,\alpha,\beta,\gamma) = 2\pi + 2\pi + 2\pi = 6\pi$, both of them hold independently on the choice of $\alpha,\beta,\gamma$. Therefore, we have

$$\begin{aligned}
\lim_{n\to\infty} \left( \max_{\alpha,\beta,\gamma\in[0,2\pi]} \frac{S(M_n)}{P(M_n,\alpha,\beta,\gamma)} \right) &= \lim_{n\to\infty} \frac{S(M_n)}{P(M_n,\alpha,\beta,\gamma)} \\
&= \frac{2}{3}
\end{aligned}$$

which proves 2). □

# 4. A RECTILINEARITY MEASURE FOR 3D MESHES

Motivated by the properties of the function

$$\max_{\alpha,\beta,\gamma\in[0,2\pi]} \frac{S(M)}{P(M,\alpha,\beta,\gamma)}$$

we define a rectilinearity measure for 3D meshes.

Definition 2. *For an arbitrary 3D mesh $M$ we define its rectilinearity $R(M)$ as*

$$R(M) = 3 \times \left( \max_{\alpha,\beta,\gamma\in[0,2\pi]} \frac{S(M)}{P(M,\alpha,\beta,\gamma)} - \frac{2}{3} \right). \quad (1)$$

According to the definitions and theorems introduced above, we obtain the following theorem which summarizes the properties of the 3D mesh rectilinearity measure proposed here.

Theorem 3. *For any 3D mesh $M$, we have:*

1. *$R(M)$ is well defined and $R(M) \in (0,1]$;*
2. *$R(M) = 1$ if and only if $M$ is rectilinear;*
3. *$\inf_{M\in\Pi}(R(M)) = 0$, where $\Pi$ denotes the set of all 3D meshes;*
4. *$R(M)$ is invariant under similarity transformations.*

# 5. COMPUTATION OF RECTILINEARITY

Unlike the computation of the accurate rectilinearity for 2D polygons [31], because of the complexity of $P(M,\alpha,\beta,\gamma)$ (see Appendix) it is difficult (maybe impossible) to calculate the exact value of rectilinearity for 3D meshes. From the introduction of preceding sections, we can see that the computation of the rectilinearity is actually a nonlinear optimization problem which can be efficiently solved by intelligent computing methods. In this paper we choose Genetic Algorithms which is an optimization technique based on natural evolution [9].

First, we define a population including $N_g$ individuals. Each individual consists of a value of fitness and three different chromosomes which are presented by binary codes. The fitness of an individual is defined as $fit(\alpha,\beta,\gamma) = \frac{S(M)}{P(M,\alpha,\beta,\gamma)}$ and rotating angles $\alpha,\beta,\gamma$ are encoded in the three chromosomes. The stopping criterion here is the number of evolution generations $N_{gen}$.

Iterating the genetic algorithm process including encoding, evaluation, crossover, mutation and decoding for $N_{gen}$ generations, we get an individual with the group's greatest fitness which can be used as the approximate value of $\max_{\alpha,\beta,\gamma\in[0,2\pi]} \frac{S(M)}{P(M,\alpha,\beta,\gamma)}$.

Finally, we calculate the rectilinearity of the mesh by Equation (1).

Note: the parameters of the Genetic Algorithm in this paper are chosen as follows. The number of individuals $N_g = 50$ and evolution generations $N_{gen} = 200$. The length of chromosome's binary codes $L_c = 20$. The probability of crossover $p_c = 0.800$ and mutation $p_m = 0.005$.

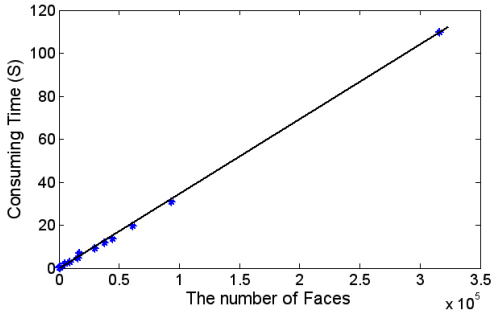


**Figure 3: The number of faces versus computation time**

# 6. EXPERIMENTAL RESULTS

Since the rectilinearity measurement proposed in this paper is calculated based on the area of triangles, together with the definitions and theorems described in the previous sections we can summarize the primary advantages (already described in section 1) of this measurement. While these four properties indicate that the rectilinearity measurement may be well suited for 3D shape analysis tasks in theory, it is necessary to demonstrate that these desirable properties are also satisfied in practice. As the third and fourth properties are obvious, in this section we only illustrate experimental results to investigate the following questions:

1. How well does this measurement correspond with the intuitive perception of rectilinear 3D shapes?
2. How robust is this measurement with respect to geometric noise and small errors or changes in topology?

We implemented the calculation of rectilinearity described in section 5 in Visual C. The experiments were run on a Windows XP Laptop with a 2.0 GHz Intel Core 2 Duo CPU, 1.0 GB DDR2 memory and an NVIDIA Quadro NVS 140M graphics card. After the parameters of the GA have been chosen, the total computing time is proportional to the number of faces. The relationship between computing time and the number of faces of some individual meshes is demonstrated in Figure 3. We can see that usually the calculation can be finished within seconds and the computing complexity is $O(N)$ where $N$ denotes the number of faces.

## 6.1 Rank of the rectilinearity

The rectilinearity measurement is applied to some meshes which are obtained from a cube-like open mesh by cutting a part of different size at a same direction. The rank of rectilinearity is shown in Figure 4. All examples show that the rectilinearity measure is well behaved.

The rectilinearity measure is now applied to a wide range of 3D meshes which are then ranked in order of decreasing rectilinearity (Figure 5). Note that the rectilinearity of cube is not exactly 1, this is because of computational error. Comparison against human intuitive notion shows that a similar ordering has been generated.

## 6.2 Robustness

It is often desirable that the shape descriptor is insensitive to noise and small extra features, and robust against arbitrary small topological degeneracies. In order to test the robustness of the calculation of this measurement, we add small amounts of noise or errors or both of them to several 3D meshes, and then compute the rectilinearity for these objects. Results (see Figure 6) show that our rectilinearity measurement of 3D meshes is robust to small errors or changes in topology and insensitive to noise, because small changes of a mesh result in small changes to its surface area and projected areas.

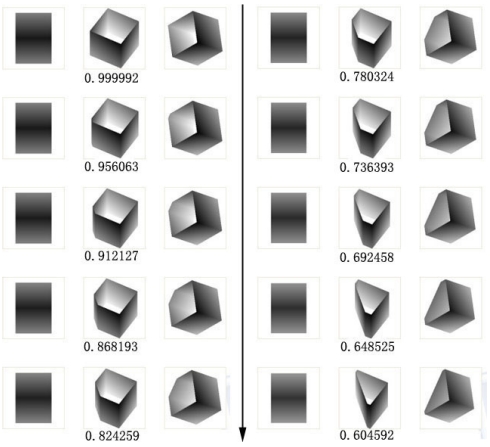


**Figure 4: 3D meshes have identical inner angles but differ in rectilinearity. All objects are displayed by images captured from three different view points. Underneath are the corresponding rectilinearity values.**

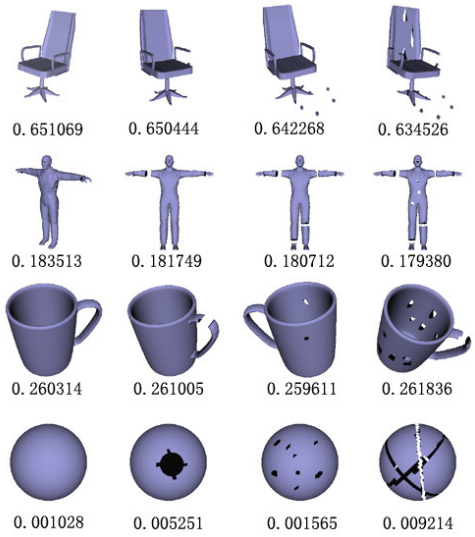


**Figure 6: Robustness of the calculation of rectilinearity. Underneath are the values of rectilinearity.**

# 7. SOME APPLICATIONS

## 7.1 Pose Normalization

The calculation of rectilinearity can be used for pose estimation of 3D meshes. The basic idea is that the value of $\alpha, \beta, \gamma$ maximising $\frac{S(M)}{P(M,\alpha,\beta,\gamma)}$ of a mesh $M$ specifies a standard pose for this object. Figure 7 illustrates some results of rectilinearity based and PCA based normalization methods, respectively.

From Figure 7 we can see that usually, from the intuitive perception of a human being, the rectilinearity based method performs better than the PCA based method, especially when processing artificial objects such as tables, chairs, houses, cabinets, etc. Moreover, what is most important is that the rectilinearity based method

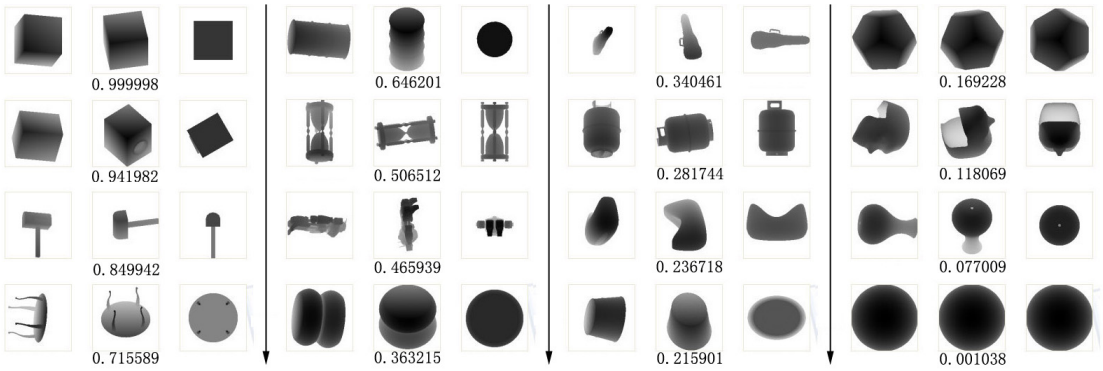


**Figure 5: Shapes ranked by rectilinearity. All objects are displayed by images captured from three different view points. Underneath are the corresponding rectilinearity values.**

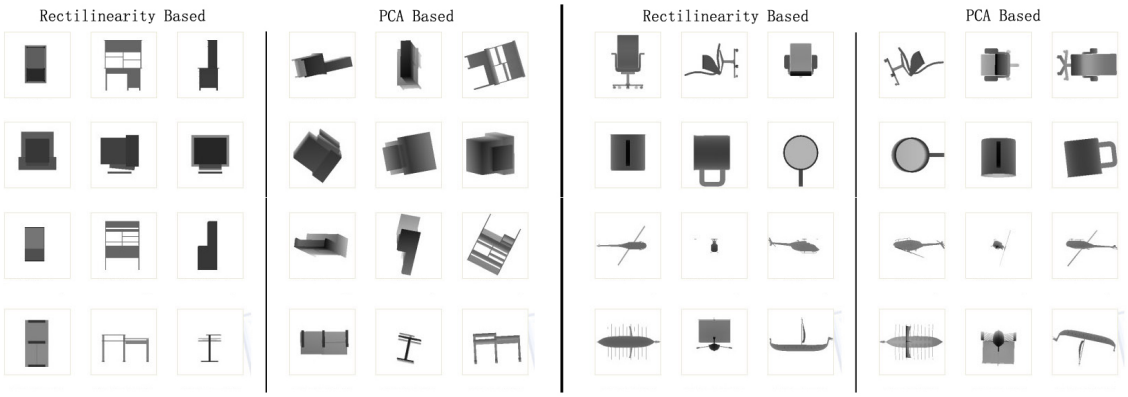


**Figure 7: Comparison of rectilinearity based and PCA based pose normalization methods. All objects are shown by three images captured from the positive directions along the $x$, $y$, and $z$ axes, respectively.**

is much more stable than the PCA based method (shown in Figure 8), because small changes in the mesh result in small changes in the areas but may result in large changes of the second order moments which are applied to calculate the principle axes in the PCA algorithm. However, there are also some models which can be perfectly registered by the PCA based method rather than our method. Therefore, a good approach may be to combine different pose normalization methods in order to be able to cope well with all (or most) shapes. This topic will be investigated in the future.

## 7.2 3D Shape Retrieval

The goal of this experiment is to evaluate the retrieval performance of the combined features consisting of the rectilinearity measurement and other three commonly used shape descriptors:

- **D1:** A histogram of distances from the center of mass to points on the surface [1]. The number of histogram bins is selected as 64.
- **D2:** A histogram of distances between pairs of points on the surface [14]. The number of histogram bins is chosen as 64.
- **LFD:** A representation of a model as a collection of depth-buffers rendered from uniformly sampled positions on a view sphere. 35 Zernike moments, 10 Fourier coefficients, eccentricity and compactness, extracted from these depth-buffers, are used as the descriptor of the model. In order to accelerate the retrieval speed, our LFD descriptor is slightly different from the original one proposed in [4]. We first normalize the objects into a canonical coordinate system using PCA algorithm, then capture 60 depth-buffers from uniformly distributed viewpoints on the unit sphere, thus construct a transformation invariant feature vector with 2820 elements.

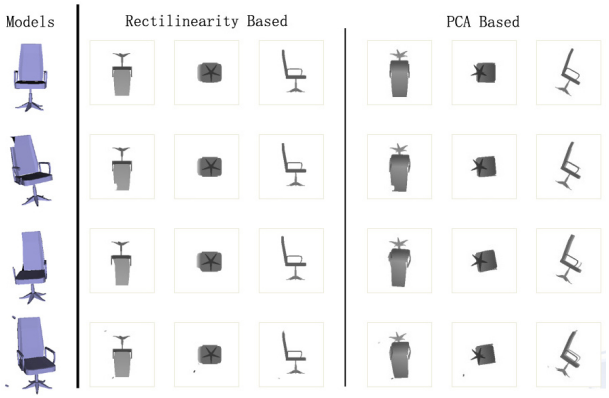


**Figure 8: Comparison of the robustness between our method and PCA based method for pose normalization. Normalization results are shown by three images captured from the positive directions along the $x$, $y$, and $z$ axes, respectively.**

There are currently several 3D model databases for performance evaluation purposes, among which, the Princeton Shape Benchmark (PSB) [21] is perhaps the most popular and well-organized. PSB is a publicly available 3D model benchmark database containing 1814 3D models which are classified into test and train sets. Here, we use the PSB test set with base classification to evaluate the retrieval performance that is quantified by the following evaluation measures:

- **Nearest neighbor (1-NN):** The percentage of the closest matches that belong to the same class as the query.
- **First-tier (1-Tier) and Second-tier (2-Tier):** The percentage of models in the query's class that appear within the top $K$ matches, where $K$ depends on the size of the query's class. Specifically, for a class with $|C|$ members, $K = |C| - 1$ for the first tier, and $K = 2(|C| - 1)$ for the second tier.
- **Discounted Cumulative Gain (DCG):** For details, we refer the reader to the paper [21].

First, we test the original descriptors on PSB separately. Results are shown in Table 1. Next, the rectilinearity values, with well tuned weights (using the train set of PSB), are added to the original signatures to form new features. Thus we obtain three new combined descriptors which are denoted as D1+R, D2+R, and LFD+R, where the weights of rectilinearity are selected as 0.53, 0.29, and 41, respectively. Retrieval results of them are demonstrated in Table 2. The distance between every pair of shape descriptors is calculated using their $L_1$ difference. We can see that considerable improvements have been achieved, mainly because the rectilinearity measure provides extra effective information with respect to the original shape descriptors.

**Table 1: Retrieval performance of three individual descriptors.**

| | D1 | D2 | LFD |
|---|---|---|---|
| 1-NN | 26.13% | 33.73% | 65.49% |
| 1-Tier | 13.12% | 16.40% | 37.15% |
| 2-Tier | 19.01% | 24.55% | 47.86% |
| DCG | 40.38% | 44.42% | 63.83% |

**Table 2: Retrieval performance of three combined descriptors. The value in the bracket means the percentage of the improvement with respect to the original one.**

| | D1+R | D2+R | LFD+R |
|---|---|---|---|
| 1-NN | 33.84%(29.54%) | 44.98%(33.33%) | 68.13%(4.04%) |
| 1-Tier | 18.68%(42.38%) | 22.44%(36.78%) | 41.05%(10.48%) |
| 2-Tier | 28.03%(47.42%) | 31.89%(29.91%) | 53.30%(11.38%) |
| DCG | 46.66%(15.54%) | 50.07%(12.71%) | 67.25%(5.37%) |

# 8. CONCLUSION

In this paper, we have proposed a novel rectilinearity measurement, describing the extent to which a 3D mesh is rectilinear, and we also proved several corresponding theorems. The measurement presented here has several desirable properties including simplicity, stability, robustness, and invariance to similarity transformation. We demonstrated how to compute it efficiently by a Genetic Algorithm. Afterward, a series of experiments were carried out to validate the robustness as well as the effectiveness of our shape measurement in practice. Finally, we conducted two application examples to show that the rectilinearity measurement not only provides a new tool to normalize the pose of 3D objects, but also significantly improves the performance of 3D shape retrieval system through the combination with other shape descriptors.

Three directions for future investigation are listed as follows:

1. Is it possible to calculate the optimal value of the rectilinearity analytically, and how can this be done?
2. Can the rectilinearity based pose normalization method be combined with the PCA algorithm to achieve better performance?
3. Can we derive other 3D shape measurements, such as convexity, rectangularity, and compactness, using the relation between area and projected areas instead of the perimeter in 2D field in the same manner as we have described in this paper?

# 9. ACKNOWLEDGEMENTS

This work was supported by China Scholarship Council and NSFC Grant 60674030.

# 10. REFERENCES

[1] M. Ankerst, G. Kastenmuller, H. P. Kriegel, and T. Seidl. Nearest neighbor classification in 3d protein databases. In *Proc. the Seventh International Conference on Intelligent Systems for Molecular Biology*, pages 34–43, 1999.

[2] E. Bribiesca. An easy measure of compactness for 2d and 3d shapes. *Pattern Recognition*, 41(2):543–554, 2008.

[3] B. Bustos, D. Keim, D. Saupe, T. Schreck, and D. Vranić. An experimental effectiveness comparison of methods for 3d similarity search. *International Journal on Digital Libraries*, 6(1):39–54, 2005.

[4] D. Y. Chen, X. P. Tian, Y. T. Shen, and M. Ouhyoung. On visual similarity based 3d model retrieval. In *Proc. Eurographics 2003*, volume 22, pages 223–232, 2003.

[5] J. Corney, H. Rea, D. Clark, J. Pritchard, M. Breaks, and R. MacLeod. Coarse filters for shape matching. *IEEE Computer Graphics and Applications*, 22(3):65–74, 2002.

[6] M. Elad, A. Tal, and S. Ar. Content based retrieval of vrml objects: an iterative and interactive approach. In *Proc. the Sixth Eurographics workshop on Multimedia 2001*, pages 107–118, 2001.

[7] T. Funkhouser and P. Shilane. Partial matching of 3d shapes with priority-driven search. In *Proc. the Fourth Eurographics symposium on Geometry processing*, pages 131–142, 2006.

[8] R. M. Haralick. A measure for circularity of digital figures. *IEEE Trans. Systems, Man, and Cybernetics*, 4:394–396, 1974.

[9] J. H. Holland. *Adaptation in Natural and Artificial Systems: An Introductory Analysis with Applications to Biology, Control and Artificial Intelligence*. MIT Press, 1992.

[10] M. Kazhdan, B. Chazelle, D. Dobkin, T. Funkhouser, and S. Rusinkiewicz. A reflective symmetry descriptor for 3d models. *Algorithmica*, 38(1):201–225, 2003.

[11] M. Kazhdan, T. Funkhouser, and S. Rusinkiewicz. Rotation invariant spherical harmonic representation of 3d shape descriptors. In *Proc. 2003 Eurographics Symposium on Geometry Processing*, volume 43, pages 156–164, 2003.

[12] J. Leou and W. Tsai. Automatic rotational symmetry determination for shape analysis. *Pattern Recognition*, 20(6):571–582, 1987.

[13] S. Loncaric. A survey of shape analysis techniques. *Pattern Recognition*, 31(8):983–1001, 1998.

[14] R. Osada, T. Funkhouser, B. Chazelle, and D. Dobkin. Shape distributions. *ACM Transactions on Graphics*, 21(4):807–832, 2002.

[15] E. Paquet and M. Rioux. Nefertiti: a query by content system for three-dimensional model and image databases management. *Image and Vision Computing*, 17(2):157–166, 1999.

[16] E. Paquet, M. Rioux, A. Murching, T. Naveen, and A. Tabatabai. Description of shape information for 2-d and 3-d objects. *Signal Processing: Image Communication*, 16(1-2):103–122, 2000.

[17] M. Petitjean. Chirality and symmetry measures: A transdisciplinary review. *Entropy*, 5:271–312, 2003.

[18] D. Proffitt. The measurement of circularity and ellipticity on a digital grid. *Pattern Recognition*, 15(5):383–387, 1982.

[19] P. L. Rosin. Measuring rectangularity. *Machine Vision and Applications*, 11(4):191–196, 1999.

[20] P. L. Rosin. Measuring shape: ellipticity, rectangularity, and triangularity. *Machine Vision and Applications*, 14(3):172–184, 2003.

[21] P. Shilane, P. Min, M. Kazhdan, and T. Funkhouser. The princeton shape benchmark. In *Proc. Shape Modeling Applications 2004*, pages 167–178, 2004.

[22] H. Sundar, D. Silver, N. Gavani, and S. Dickinson. Skeleton based shape matching and retrieval. In *Proc. Shape Model. Int. 2003*, pages 130–139, 2003.

[23] J. W. Tangelder and R. C. Veltkamp. A survey of content based 3d shape retrieval methods. *Multimedia Tools and Applications (in press)*.

[24] J. W. H. Tangelder and R. C. Veltkamp. Polyhedral model retrieval using weighted point sets. In *Proc. Shape Modeling International 2003 (SMI'03)*, pages 119–129, 2003.

[25] D. V. Vranić and D. Saupe. 3d model retrieval. In *Spring Conference on Computer Graphics and its Application (SCCG2000)*, pages 89–93, 2000.

[26] D. V. Vranić, D. Saupe, and J. Richter. Tools for 3d-object retrieval: Karhunen-loeve transform and spherical harmonics. In *Proc. 2001 IEEE Fourth Workshop on Multimedia Signal Processing*, pages 293–298, 2001.

[27] Y. Yang, H. Lin, and Y. Zhang. Content-based 3-d model retrieval: A survey. *IEEE Trans. Systems, Man, and Cybernetics*, 37(6):1081–1098, 2007.

[28] C. Zhang and T. Chen. Efficient feature extraction for 2d/3d objects in mesh representation. In *Proc. ICIP 2001, Thessaloniki, Greece*, volume 3, pages 935–938, 2001.

[29] C. Zhang and T. Chen. Indexing and retrieval of 3d models aided by active learning. In *Proc. ACM Multimedia*, pages 615–615, 2001.

[30] D. Zhang and G. Lu. Review of shape representation and description techniques. *Pattern Recognition*, 37(1):1–19, 2004.

[31] J. Žunić and P. L. Rosin. Rectilinearity measurements for polygons. *IEEE Trans. Pattern Analysis and Machine Intelligence*, 25(9):1193–1200, 2003.

[32] J. Žunić and P. L. Rosin. A new convexity measure for polygons. *IEEE Trans. Pattern Analysis and Machine Intelligence*, 26(7):923–934, 2004.

# APPENDIX

LEMMA 1. *$\frac{P(M,\alpha,\beta,\gamma)}{S(M)}$ is a nonconstant function defined on $\alpha,\beta,\gamma \in [0,2\pi]$.*

PROOF. We prove the lemma by a contradiction: $\frac{P(M,\alpha,\beta,\gamma)}{S(M)}$ is a constant function defined on $\alpha,\beta,\gamma \in [0,2\pi]$. Assume that the unit normal of the triangle $T_i$ is $n_i = [a_i, b_i, c_i]^T$. After rotation, we obtain a new normal

$$n_i' = R(\alpha,\beta,\gamma)n_i = \begin{bmatrix} a_i' \\ b_i' \\ c_i' \end{bmatrix}$$

where

$$\begin{aligned} a_i' &= a_i\cos\gamma\cos\beta + b_i(\sin\gamma\cos\alpha + \cos\gamma\sin\beta\sin\alpha) \\ &\quad + c_i(\sin\gamma\sin\alpha - \cos\gamma\sin\beta\cos\alpha) \\ b_i' &= -a_i\sin\gamma\cos\beta + b_i(\cos\gamma\cos\alpha - \sin\gamma\sin\beta\sin\alpha) \\ &\quad + c_i(\cos\gamma\sin\alpha + \sin\gamma\sin\beta\cos\alpha) \\ c_i' &= a_i\sin\beta - b_i\cos\beta\sin\alpha + c_i\cos\beta\cos\alpha. \end{aligned}$$

And we have

$$\frac{P(M,\alpha,\beta,\gamma)}{S(M)} = \frac{\sum_{i=1}^{N}(|a_i'|S_i + |b_i'|S_i + |c_i'|S_i)}{\sum_{i=1}^{N} S_i}$$

Let $\alpha,\beta$ be constants and ensure that not all faces of the mesh are parallel to XOY plane. Then we can find an interval $\gamma \in [\gamma_0, \gamma_0 + \varepsilon], \varepsilon > 0$ such that

$$P(M,\alpha,\beta,\gamma) = \sum_{i=1}^{N}(fa_i \cdot a_i' \cdot S_i + fb_i \cdot b_i' \cdot S_i + fc_i \cdot c_i' \cdot S_i)$$

and

$$\begin{aligned} &P_{YOZ}(M,\alpha,\beta,\gamma) + P_{ZOX}(M,\alpha,\beta,\gamma) \\ &= \sum_{i=1}^{N}(fa_i \cdot a_i' \cdot S_i + fb_i \cdot b_i' \cdot S_i) > 0 \end{aligned}$$

where $\{fa_i, fb_i, fc_i | i = 1,2,\ldots,N\} \subset \{+1,-1\}$.
Since $\frac{P(M,\alpha,\beta,\gamma)}{S(M)}$ and $S(M)$ both are constant functions, $P(M,\alpha,\beta,\gamma)$ should also be a constant function defined on $\alpha,\beta,\gamma \in [0,2\pi]$. Then we obtain

$$\begin{aligned} 0 &= \frac{d(P(M,\alpha,\beta,\gamma))}{d\gamma} = \frac{d^2(P(M,\alpha,\beta,\gamma))}{d\gamma^2} \\ &= \sum_{i=1}^{N}(-fa_i \cdot a_i' \cdot S_i - fb_i \cdot b_i' \cdot S_i) < 0 \end{aligned}$$

when $\alpha,\beta$ are the given constants and $\gamma \in [\gamma_0, \gamma_0 + \varepsilon], \varepsilon > 0$. The obtained contradiction $0 < 0$ proves the lemma. □